Int. j. adv. multidisc. res. stud. 2024; 4(5):125-133

Received: 19-07-2024
Accepted: 29-08-2024

International Journal of Advanced Multidisciplinary Research and Studies

ISSN: 2583-049X

Laser Non-Destructive Test to Find Aluminum Metal Physical Properties

Narjis Z Abdulzahra
Department of Physics, College of Sciences, Al-NahrainUniversity, Jadriya, Baghdad, Iraq

DOI: https://doi.org/10.62225/2583049X.2024.4.5.3202
Corresponding Author: **Narjis Z Abdulzahra**

Abstract
Laser shock penning is a non-destructive laser testing used for analyzing material using lasers without causing damage, offering valuable insights into material properties; a recent experimental study focused on examining the al physical characteristics achieved by utilizing high-resolution optical microscopy and SEM images and investigated the effects of varying energy levels of Nd: Yag laser particularly analyzing the track effects the shock wave velocity was observed to depend on the surrounding medium influencing the ionization rates of the atoms involved notably Al subjected in water and ethanol exhibited a shock pressure of 4.5 GPa contrasting with the typical range of 0.46 to 3.2 GPa (in air, water, and ethanol environments) at a measuring laser intensity 11.4 GW/cm², This method was utilized for examining shock characteristics, encompassing particle speed, shock duration wavelength, energy strength, loudness level, and force, which were then used for assessing mechanical characteristics and juxtaposed with conventional methods. For example, tensile tests for stress-strain and Vickers hardness indicated that shocked Al in water and ethanol environments showed a closer correlation with tensile test results; in contrast, water demonstrated better alignment with Vickers hardness measurements. Additionally, there were discrepancies in elastic modulus values between tensile tests 28 GPa, and by laser shock, peening is 8.4 GPa, 4.9 GPa, and 4.7 GPa in air, water, and ethanol environments, respectively.

Keywords: Laser-Induced Shock Pressure Generates Particle Velocity, Parameters of the Shock Wave, NDLT

1. Introduction

Laser-induced shock waves (LISP) make modifications and change material characterization because ultra-intensity lasers generate intense shock waves that can alter material properties [1].

The phenomenon involves heating the aluminum surface with a high-power laser pulse, causing vaporization and expansion. A laser creates a high-pressure shock wave, leading to ablation, melting, and deformation, depending on laser parameters and material properties. The shock wave may also eject particles or debris from the surface. Control over laser parameters enables precise manipulation of these effects [2, 3].

Applications of laser-induced shock waves in Al include shaping, modification, and cleaning surfaces, which are essential in industries like aerospace and microelectronics. Variations in shock wave characteristics arise from experimental setups and laser parameters, driving ongoing research to enhance understanding and industrial application [4].

The formula that highlights technical specific surface temperature after a derived formula gives laser-induced shock wave processing [5].

$$T_{(0,t<\tau)} = \frac{2\alpha I_0(1-R)}{K_{th}}\sqrt{\frac{Dt}{\pi}} \quad (1)$$

The absorption coefficient (α), laser peak power (I0), reflectivity at 1.064μm (R), and thermal diffusivity are given as D=K_{th} ρc_p. (K_{th}) is the thermal conductivity, density (ρ), and specific heat (c_p) can calculate the temperature grade (in degrees Celsius per centimeter) [4, 8]. Finally, The Al properties used in this context are specified as Table 1.

Table 1: Shows Al and media properties, including density, Thermal conductivity, Thermal diffusivity, and Specific heat [5-9]

Medium	Density (Kg/m^3)	Thermal conductivity (W/(m.K)	Thermal diffusivity $\times 10^{-6}$ (m^2/s)	Specific heat (KJ/Kg.K)
Air	1.2	0.03	20	1
Water	1000	0.6	0.14	4
Ethanol	790	0.18	0.1	2.3
Al	2710	204	80	1

Table 2: Al and media properties, optical absorption coefficient, and Reflectivity at a wavelength at (1.064µm) [5-9]

Medium	Absorption coefficient(cm^{-1})	Reflectivity
Air	-	-
Water	10^4	0.02
Ethanol	105	0.023
Al	1.24×10^6	0.95

The Study investigates shock wave parameters of Al metal under various experimental conditions, including different media such as air, water, and ethanol. The research focuses on establishing model boundary values and developing practical methods for tracking laser spots to assess the mechanical characteristics of various materials.

2. Experimental Methods

The LSP process depends on several factors, including the target material and laser type, as well as the properties of the absorbent and transparent overlay. The current study compares the non-distractive method (data derived from optical images) versus traditional measurements to find mechanical properties.

2.1 Resource Objectives

The study describes using a 2 mm thick aluminum alloy 2024 target. The cleaning procedure included the use of ethanol in an ultrasonic cleaner. Subsequently, it was polished using different grades of polishing paper, starting with coarse grit and progressing to finer ones (1500, 300, 180, and 120 grit). The metal was subsequently cut into a 3×3 cm^2 square to improve laser absorption. X-ray diffraction analysis offers valuable information regarding the crystal structure, chemical composition, and physical characteristics of the material. The analysis of X-ray radiation scattering on a sample under various conditions presents X-ray analysis results for Al. Based on Bragg's law, it explains the scattering of primary electrons when X-ray waves interact with materials [6].

$$d = n\lambda/2\sin\theta \quad (2)$$

Where (d) is the interplanar spacing, (θ) is the incident angle, n represents the diffraction order, and (λ) is the X-ray wavelength. The relation of (d) and lattice constant (a) is given by [6, 7]:

$$a = d/\sqrt{h^2 + k^2 + l^2} \quad (3)$$

The Al volume is given by :

$$V = a^3 \quad (4)$$

Al density equal to [7]:

$$\rho = nM/V.A_v \quad (5)$$

In this equation, ρ density in (g/cm^3), n represents the atom number for a face-centered cubic FCC with 4, the atomic weight of the material M, the volume V, and the Avogadro constant(Av). The calculated density is 2.279 g/cm^3.

The mechanical tensile test of the used material was fabricated according to the dimensions specified in ASTM E8/E8m-13a, with an Al specimen length greater than four times the diameter. Vickers Digital Micro test was employed for testing using the " Vickers Hardness Tester type TH714" under various applied loads (0.49N, 0.98N, 1.96N, 2.94N, and 4.9N).

2.2 Laser

Our experimental studies employ the laser Nd: YAG operated at 1.064 µm. This particular laser, manufactured by DELIXI, is utilized in our research to deliver pulse energies spanning 50 to 500 millijoules over a pulse duration of 7 nanoseconds. The temporal profile of the pulses follows a Gaussian distribution, as shown in Fig 2.

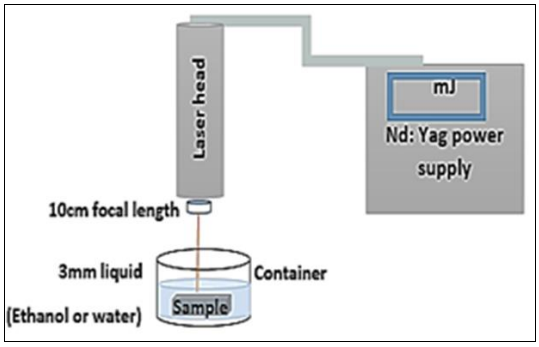

Fig 2: The configuration for the experiment involves utilizing Nd: YAG laser with a focal lens of 10 cm

A 10cm focal lens concentrates the laser beam onto Al, which has a diameter of 0.08 cm. The laser system features a closed cooling mechanism. The computed intensity laser of (I) is according to established methods [8, 9].

$$I = \frac{E}{At_p} \quad (6)$$

The laser energy (E in joules), pulse duration (7 ns), and laser spot area. The laser intensity values can be referenced in Table 3.

Table 3: Laser intensity at different laser energies

Laser energy (m J)	I (GW/cm^2)
50	1.43
100	2.86
150	4.29
200	5.71
250	7.14
300	8.57
350	10
400	11.43

3. Results

3.1 The heating temperature of Al after the laser shot

Fig (3) Illustrated the relationship between temperature and laser intensity. The correlation between increasing temperature and laser intensity is evident, as equation (1) describes. When utilizing the laser of Nd: YAG on an Al immersed in an ethanol liquid, Al temperature increases compared to Al submerged in water. This variation can be ascribed to ethanol and water's distinct physical properties and behaviors as cooling agents [9]. Ethanol exhibits a lower thermal conductivity than water, reducing its efficacy in dissipating heat from the Al surface. Consequently, when the Nd: YAG laser is applied, the Al surface experiences a slightly more significant temperature rise.

Furthermore, ethanol's lower boiling point facilitates evaporation at higher temperatures, which absorbs heat from the surface and diminishes its cooling effect compared to water.

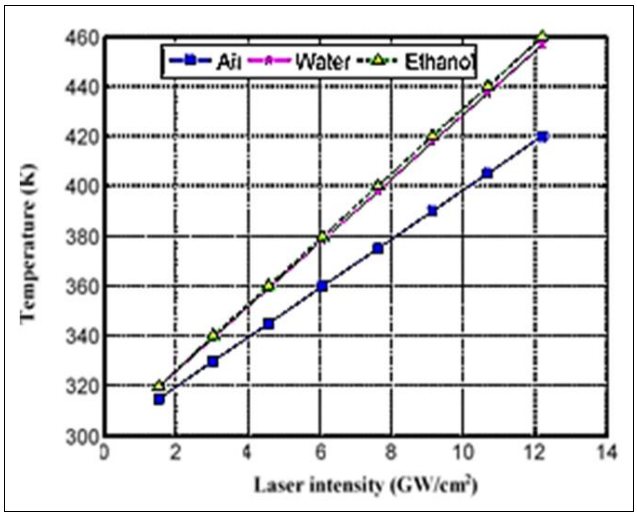

Fig 3: Measurements of Al surface temperature vary across different laser intensities

3.2 Surface Topography

LSP technology uses powerful laser pulses to create shock waves within a material, which changes its structure [10]. This study examined how aluminum responded to laser treatment using an Nd-yag laser at different strengths. Then, high-resolution optical and SEM were used to study laser effects on Al surface structure. The SEM images showed different areas affected by the laser. In particular, a pillar-like structure was more noticeable when ethanol was used. This was because ethanol conducts heat well and can dissipate heat quickly, affecting how the laser impacted the aluminum. Additionally, ethanol's flammability caused the laser's impact variations under different temperatures. The process of removing material with the laser involves both heat and chemicals. Lower laser strengths heat the material, while higher strengths melt it, causing the material to be removed through vaporization. The vaporized material forms a plume, often taking on a slightly conical or cylindrical shape [11, 12].

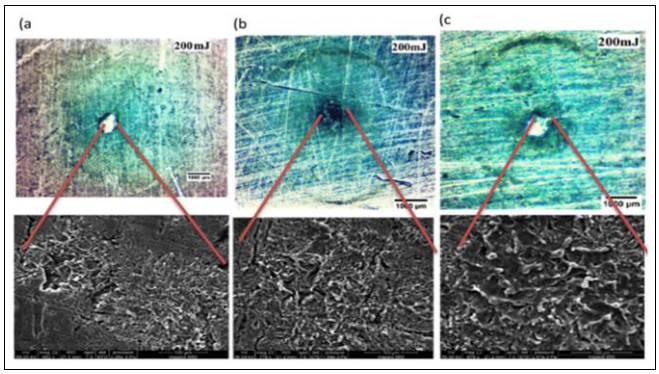

Fig 4: Laser-induced shockwave phenomena generated by directing laser energy of 200mJ onto Al in different mediums: (a) air, (b) water, and (c) ethanol

3.3 Shock Pressure

The plasma expansion creates a recoiling pressure wave reaching gigapascal (GPa) levels after the laser incident on Al, exceeding the material's dynamic yield strength. Fabbro *et al.* [13] developed an analytical model for generating shock waves using a laser intensity with high intensity (Io). This model highlights the shock wave's effect, especially with a large Gaussian laser beam [13, 14].

$$P = 32.2\left[\frac{\alpha}{2\alpha+3}\right]^{1/2} \rho_0^{1/2} (I)^{2/3} \quad (7)$$

$$Z = \rho_0 . V_l \ . \quad (8)$$

$$\frac{2}{\rho_0^{1/2}} = \frac{1}{\rho_1^{1/2}} + \frac{1}{\rho_2^{1/2}}. \quad (9)$$

Where (Z) represents acoustic impedance, which varies with the characteristics of the restraining intermediate (z_1) and the used target (z_2). The total density (ρ_0) represents the combined density of the medium, with the confining medium (ρ_1) and target material density (ρ_2) contributing accordingly. Laser intensity (I), measured in GW/cm^2, plays a crucial role in converting internal energy to thermal energy ($\alpha \approx 0.25$) [14, 15].

Fig 5 illustrates how increasing laser intensity elevates shock pressure by rapidly imparting higher energy to the liquid. Consequently, a more potent shock wave ensues, resulting in heightened pressure. Notably, the acoustic pressure in liquefied (e.g., water, ethanol) surpasses that in a gas medium (such as air). This discrepancy arises from the higher density of liquids, attributed to their molecular proximity. The closer molecular arrangement in liquids leads to a denser volume, yielding higher confrontation. The laser intensity (GW/cm^2) and shock pressure (GPa) were measured as detailed in Table 4.

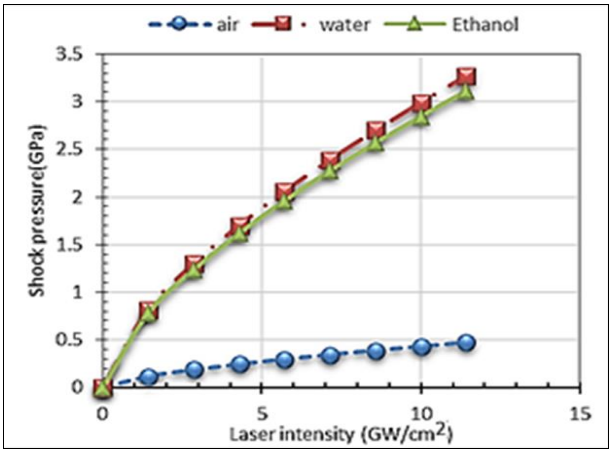

Fig 5: The correlation between laser intensity and shock pressure

Table 4: Laser intensity (GW/cm^2) VS. shock pressure (GPa)

Laser intensity	air	water	ethanol
1.4	0.19	1.3	1.2
2.9	0.24	1.7	1.6
4.3	0.29	2.1	2.0
5.7	0.34	2.4	2.3
7.1	0.39	2.7	2.6
8.6	0.43	3.0	2.8
10.0	0.47	3.3	3.1
11.4	0.19	1.3	1.2

3.4 Media Effects on Shock Wave Dynamics

The pressure and shock particle velocities given by [3]:

$$P = \rho . V_l . V_p \quad (11)$$

Fig 6 shows that shock pressure rises across different media as particle velocity increases due to higher surface temperatures and ion release from the irradiated surface. Aluminum experiences greater pressure in liquid media than air because denser media facilitate faster shock wave transmission. Water's cohesion and ethanol's similar properties enhance resistance to forces, resulting in higher shock pressures. The change in particle velocity with confinement media is due to density differences, acoustic impedance mismatches, and cooling effects. Denser media like water and ethanol reduce energy reflection, sustain higher velocities, and efficiently transfer energy [16, 17].

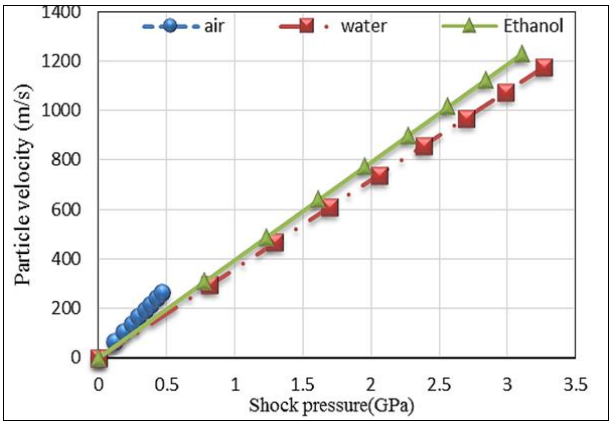

Fig 6: The relationship between shock pressure and particle velocity

3.5 The Shock length and time

The spacing between points on consecutive waves named as shock wavelength given by (Lsh or λsh) characterizes [13, 18-21]:

$$V_l = \frac{L_{sh}}{t_{sh}}. \quad (12)$$

V_l referred to as the shock velocity, is accompanied by L_{sh}, the separation between reflected waves, and TSH, which is the shock duration. Increased shock pressure infuses more energy into the material, causing pronounced deformation and compression. Figure 7(a) shows that shock wavelength escalates with rising shock pressure, resulting in denser regions that impede wave propagation. This effect is notable in water and ethanol due to higher refractive indexes and absorption properties than in air. Figure 7(b) indicates that shock time when shock Al in air is longer than in liquid media due to lower density and slower wave propagation. Liquids like ethanol and water impose higher resistance and shorter shock duration due to their elevated density and viscosity, limiting wave expansion and interaction time with the aluminum target [10, 20-22].

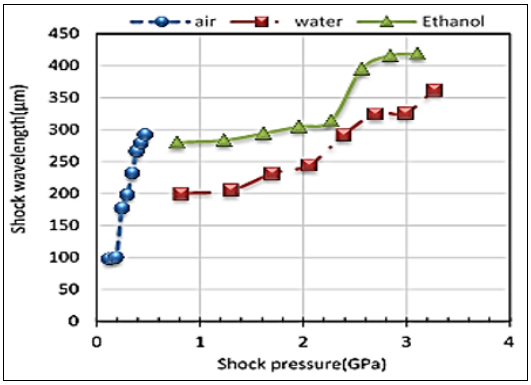

a)

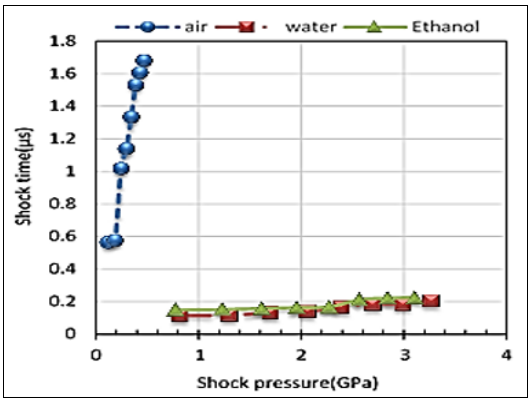

b)

Fig 7: The relationship between shock pressure and (a) shock wavelength, as well as (b) shock time across various media

Table 5 illustrates the extended duration of shock experienced by Al under Nd: YAG laser impact in ambient, as opposed to in liquids, because of the variations in density and viscosity. These variances influence the velocity of shockwave propagation and the resistance it encounters.

Table 5: Variations in media yield diverse laser intensities (measured in GW/cm²) and shock time (in µs)

Laser intensity	air	water	ethanol
2.9	0.56	0.11	0.15
4.3	0.57	0.12	0.15
5.7	1.02	0.13	0.16
7.1	1.14	0.14	0.16
8.6	1.33	0.16	0.17
10.0	1.53	0.18	0.21
11.4	1.60	0.18	0.22

3.6 Shock Wave Energy and Intensity

The shockwave energy is related to shock pressure by [22]

$$E_{sh} = P_{sh} . V \quad (13)$$

Where

$$V = \frac{4}{3} \times \pi \times r^3 \quad (14)$$

And(r) is the laser spot radius. Intensity (I_{sh}) quantifies energy flow across an area perpendicular to wave travel, expressed by dividing power by unit area [23].

$$I_{sh} = \frac{P_{sh}}{A} = \frac{E_{sh}}{A \times t_{sh}} \quad (15)$$

Compression and amplification mechanisms involve the shock wave inducing compression and deformation in aluminum, with more pronounced effects at higher pressures. Material behavior shows the elastic response at lower pressures, aiding energy transmission. Nonlinear effects at higher pressures, such as wave steepening and shock front curvature, further escalate shock intensity.

The saturation effect in aluminum at 5.7 GW/cm² laser intensities results from alternating stresses, ion influences, and pressures. Ultrasonic wave intensity relates to acoustic pressure, impedance, and particle vibration. Shock intensity varies due to transmission conditions and media differences, including wave scattering, absorption, and mechanical energy transmission [24].

The saturation effect in Fig. 8(a) depends on experimental conditions and the Al sample, with elastic behavior and nonlinear effects increasing shock intensity. Fig. 8(b) shows shock energy escalation due to absorption, reduced sound scattering, and mechanisms like energy transfer, compression, and material behavior in aluminum.

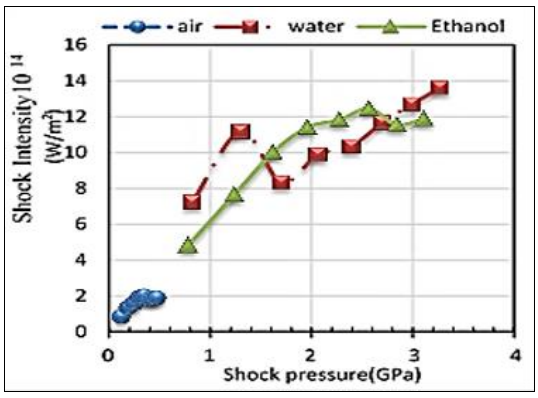

a)

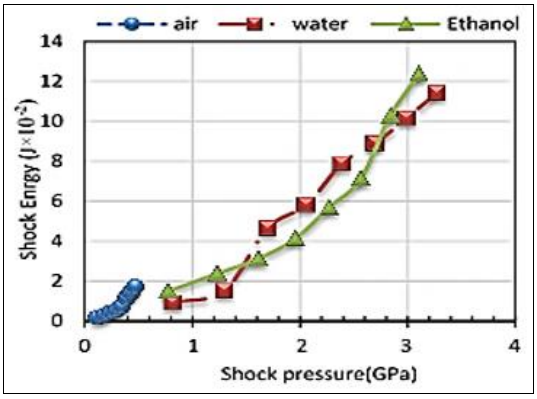

b)

Fig 8: The correlation between Shock pressure with (a) shock intensity and (b) shock energy across varies across different media

3.7 Noise Volume Level and Shock Amplitude

The logarithm of intensity measures shock loudness (I0), with the hearing threshold at 10^{-12} W/m². Sound intensity level is defined as [25, 26]:

$$\beta = (10\text{dB}) \log\left(\frac{I}{I_0}\right). \quad (16)$$

Decibels (dB) represent loudness, which requires a tenfold power increase to sound twice as loud. The shock amplitude (P_A) related to power intensity (I_{sh}):

$$I_{sh} = \frac{P_A^2}{2\rho \times V_l}. \quad (17)$$

Density (ρ) influences this relationship. Figure 9(a) indicates that as shock pressure increases, shock loudness also rises because of affected impedance mismatches between mediums. Denser mediums like water and ethanol conduct sound better, enhancing shock wave energy transmission and noise propagation, with impedance differences between Al and surrounding mediums amplifying shock loudness. Water and ethanol's absorption properties differ from the air, reducing attenuation at specific frequencies and enhancing sound propagation and loudness. Figure 9(b) shows that increased shock pressure raises shock amplitude, causing greater disturbances and perceived loudness in the surrounding medium [27- 29].

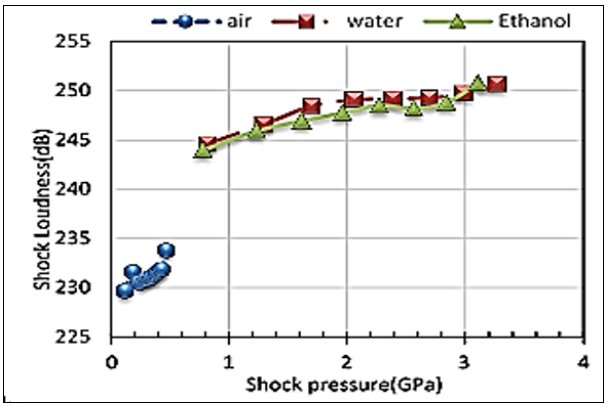

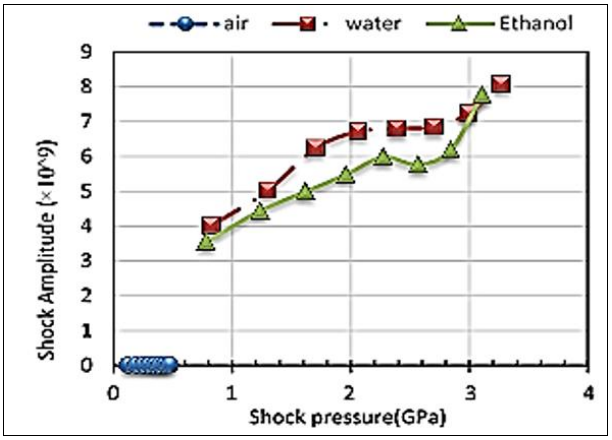

Fig 9: Shows the experimental shock pressure visualization, showcasing (a) loudness and (b) shock amplitude

3.8 Shock Wave Force and Intensity

Fig 10 illustrates that the intensity of shock wave rises with pressure in liquids due to enhanced cavitation bubble pulsation and mass transfer effects. Prolonged ultrasonic shocks reduce cavitation bubble resonance radius, lowering intensity, removal rate, and shock force. High frequencies limit bubble growth, reducing liquid disruption. Surface roughness causes resolution loss due to energy reflection and pulse expansion during transmission [12, 19].

Table 6 details experimental force values. When Al is exposed to the laser in liquids rather than air, the shock force increases with higher intensity. This results from impedance matching, which enhances energy transmission efficiency in denser mediums like water or ethanol. Better acoustic coupling in these mediums facilitates the effective transfer of energy from the shock wave to the material, amplifying the shock force [24, 30].

Table 6: Al was taken aback by the varying laser intensity levels (GW/cm^2) and shock force (kN) across different media

Laser intensity	air	water	ethanol
2.9	0.06	0.41	0.39
4.3	0.09	0.65	0.62
5.7	0.12	0.85	0.81
7.1	0.15	1.03	0.98
8.6	0.17	1.19	1.13
10.0	0.19	1.35	1.28
11.4	0.21	1.49	1.42

3.9 Mechanical Measurements

3.9.1 Shock Pressure -Strain analysis

The shock wave induces residual stress, altering the material's properties and structure.LSP is a promising alternative to conventional shot peening (SP), generating deeper and more uniform remaining stress on the target surface, up to 5 times greater [20]. The strain (ε) quantifies material deformation:

$$\varepsilon = \frac{L-L_0}{L_0} = \ln\frac{A_0}{A} \quad (18)$$

A_0 spot area and A is the interaction range. Acoustic wave velocity relates to Young's Modulus (E) [3, 15].

$$V_1 = \sqrt{\frac{E}{\rho_0}} \quad (19)$$

In various media, density (ρ) and Hooke's law correlate with stress (σ) and strain and Young's Modulus [16]:

$$\sigma = \epsilon . E \quad (20)$$

NDLT provides insights into the mechanical properties of materials through laser surface modification (LSM) and laser shock peening. This technology is widely applied across various materials. Fig 11 shows increased strain with laser shock pressure due to grain refinement and microstructural changes [15, 16]. Aluminum (Al) deforms under shock waves, experiencing greater compressive forces with increasing shock pressure, leading to heightened strain [31]. Beyond the Hugoniot Elastic Limit (HEL), Al undergoes plastic deformation and permanent strain. High shock pressures may cause wave steepening and nonlinear behavior in Al.

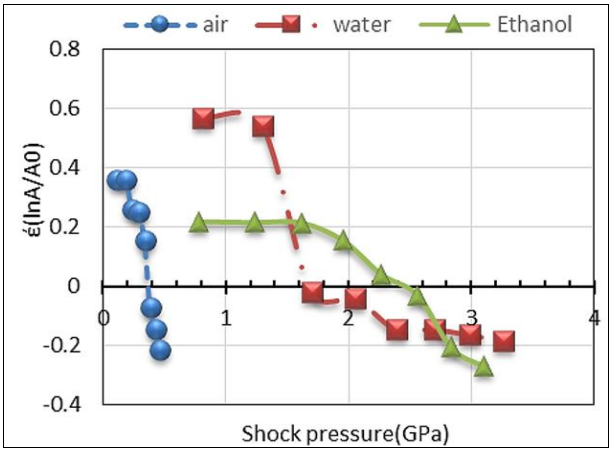

Fig 11: Strain vs. Shock pressure relationship

3.9.2 Stress

Two methods are employed for stress measurement: LSP tanique Figure (12a) and direct tensile testing Figure (12b). In LSP tanique, stress levels increase in water and ethanol compared to air due to interactions generating dislocations and microstructural deformation. This creates compressive residual stresses, which decrease away from the surface [15]. High-power pulses shock the surface, causing plastic deformation and higher dislocation density. In tensile testing, the stress-strain curve is Gaussian due to higher loads over time, leading to fractures in aluminum. LSP generates shock waves rapidly (ns) to a depth of up to 200µ using an Nd: YAG laser.

3.9.3 Elastic Modulus

Determining Elastic Modulus is essential in material analysis and is established through the LSP technique and from classical tensile stress-strain curve Figure (11b). The tensile test method yields a value of 28 GPa, while the Young's Modulus obtained via LSP is shown in Table 5. A higher Young's Modulus is observed in denser liquid media when Al is shocked in air and liquid media. This is due to increased compression and confinement from the higher density of these mediums than air, resulting in a stiffer response. Additionally, the difference in acoustic impedance between aluminum and denser mediums enhances stiffness, further increasing Young's Modulus.

Table 7: The elastic modulus (in GPa) of an Al alloy subjected to laser shot peening in different media

Media	air	Water	Ethanol
Elastic Modulus (GPa)	0.08	4.9	4.7

3.9.4 Hardness

Hardness measures a material's resistance to penetration or scratching, while strength refers to its ability to withstand external loads. Strength is divided into yield strength, the maximum stress within the elastic region, and ultimate strength, the maximum stress before fracture. The equation for hardness (H) is provided by reference [9]:

$$H = \frac{F}{A} \quad (21)$$

Figures 13(a) and 13(b) show increased hardness due to increased applied force due to work or strain hardening. Aluminum (Al) 's internal structure changes when it undergoes external force or deformation. Dislocations within the crystal lattice move and interact, creating barriers that hinder further dislocation movement, thus increasing hardness. As applied force increases, more dislocations are produced, enhancing Al's strong point and hardness [3].

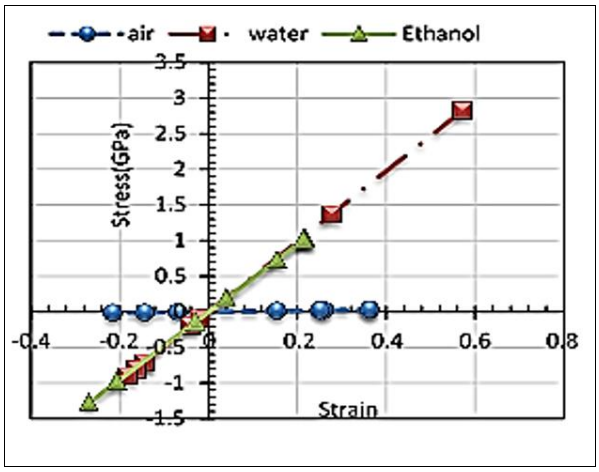

(a)

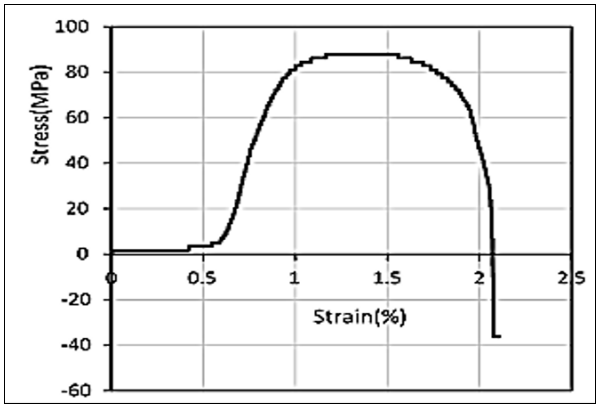

(b)

Fig 12: The stress-strain measurements utilizing the LSP technique and a tensile test

In Figure 13(a), the Al hardness is significantly higher when Al is immersed in liquids than air. The average hardness is 6.4 times higher in water and six times higher in ethanol. This can be attributed to several factors [27]: Confinement Effects: restricts dislocation movement, making the material more resistant to deformation; Increased Cooling Rate: Liquids enable faster cooling, which encourages the development of metastable phases or amorphous arrangements that are typically more rigid than the stable crystalline form; Pressure Effect: High-pressure conditions generated during shock in a liquid medium can induce phase transformations or dislocation generation, increasing hardness; Lubrication Effects: Liquids act as lubricants between grains, reducing friction and hindering dislocation movement; Enhanced Heat Dissipation: Liquids improve heat dissipation during laser shock, preventing excessive thermal softening and preserving hardness.

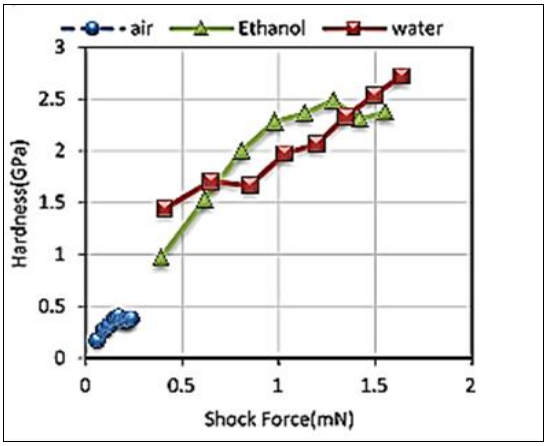

(a)

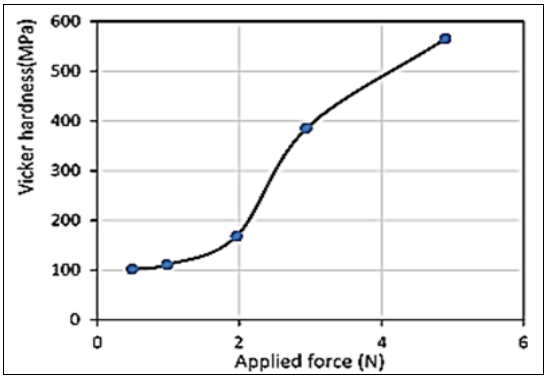

(b)

Fig 13: The hardness measurements were obtained through two distinct methods: (a) employing the LSP technique and (b) utilizing Vickers hardness testing

LSP of Al in water corresponds closely to Vickers hardening compared to other media. In air, the absence of a confining medium leads to rapid thermal cycling, inducing thermal softening and decreasing hardness. Ethanol's lower heat capacity reduces hardness due to inefficient heat dissipation, while water enhances cooling rates and pressure, increasing hardness through phase transformations and dislocations [8, 15].

In Figure 13(b), the increase in Vickers hardness for aluminum with rising applied weight is due to deformation beneath the indenter, which causes dislocations within the crystal lattice that impede atomic movement. Higher loads generate more dislocations, further enhancing hardness [3, 20, 32, 33].

4. Conclusions

This study investigates shock wave generation and pressure evaluation in direct and confined shock scenarios, comparing results with classical measurements. Data from NDLT reveal peak pressures of 0.46 to 3.2 GPa for air, water, and ethanol under 11.4 GW/cm² laser intensity. The duration of pressure application is shorter with aluminum in liquids. A transparent layer enhances shock pressure significantly. Shock propagation in water aligns closely with classical measurements, indicating that particle velocities in water and ethanol are more effective than in air. Mechanical properties such as strain and stress match better in water and ethanol, and hardness profiles from Vickers and NDLT show that water provides hardness values closer to Vickers than air or ethanol. Laser Shock Peening (LSP) proves effective for measuring mechanical properties influenced by acoustic shocks, offering a simple and cost-effective approach.

5. Acknowledgments

The author extends sincere gratitude to everyone who contributed to the completion of this research.

6. References

1. Peyre P, Berthe L, Fabbro R. Laser shock processing of materials: Basics mechanisms and applications. In *65th Meeting of Japon Laser Processing Society*. Japon Laser Processing Society, 2005. https://www.researchgate.net/publication/285589109_Laser_shock_processing_of_materials_Basics_mechanisms_and_applications
2. Claue AH, Holbrook JH, Fairand BP. Effects of laser induced shock wave. In *International Conference on Metallurgical Effects of High-Strain-Rate Deformation and Fabrication*. Shock Waves and High-Strain-Rate Phenomena in Metals, 1980, 675-702. Doi: https://doi.org/10.1007/978-1-4613-3219-0_38
3. Abdulzahra NZ. Non-Distractive Testing and Alloying by Nanosecond Nd Laser Technique as Alternative Method to Find Nano-ZnO/Al Different Properties. Laser Manufacturing and Material Processing. 2023; 10:522-547. Doi: https://doi.org/10.1007/s40516-023-00218-5
4. Yadav MJ, Jinoop AN, Danduk C, Subbu SK. Laser Shock Processing: Process Physics, Parameters, and Application. Materials Today: Proceedings. 2017; 4(8):7921-7930. Doi: https://doi.org/10.1016/j.matpr.2017.07.128
5. Abdulzahra NZ. Assessment of Surface Modification by Laser Studies of Polymer Material before and after M.B. Doping. New Trends in Physical Science Research. 2022; 1:123-132. Doi: https://doi.org/10.9734/bpi/ntpsr/v1/2097A
6. Berthe L, Fabbro R, Peyre P, Tollier L, Bartnicki E. Shock waves from a water-confined laser-generated plasma. J. Appl. Phys. 1997; 82:2826-2832. Doi: https://doi.org/10.1063/1.366113
7. Hamoudi WK, Raouf DN, Zamil N. Laser-Induced Shock Wave Studies of Para and Ferro Magnetic Materials. J. Mater. Sci. Eng. 2017; 6(3):1000349. Doi: https://doi.org/10.4172/2169-0022.1000349
8. Abdulzahra NZ. Investigation on the Surface Properties of Al after Nd Laser Nanosecond Technique in Some Media. Vidya Bharati International Interdisciplinary Research Journal (Special Issue), 2021, 738-745.
9. Callister WD. Materials Science and Engineering: An Introduction. John Wiley & Sons, Inc., 2018. https://ftp.idu.ac.id/wp-content/uploads/ebook/tdg/TEKNOLOGI%20REKAYASA%20MATERIAL%20PERTAHANAN/Materials%20Science%20and%20Engineering%20An%20Introduction%20by%20William%20D.%20Callister,%20Jr.,%20David%20G.%20Rethwish%20(z-lib.org).pdf
10. Rossing TD, Moore RF, Wheeler PA. The Science of Sound, 3rd ed. Pearson Education, Inc., 2002. https://books.google.iq/books/about/The_Science_of_Sound.html?id=W0-pBwAAQBAJ&redir_esc=y
11. Kahrizi M. Micromachining Techniques for Fabrication of Micro and Nano-Structures (InTech), 2012, 39-40. https://doi.org/10.5772/1364
12. The International Atomic Energy Agency. Ultrasonic Testing of Materials at Level 2A. Vienna, 1988. https://inis.iaea.org/collection/NCLCollectionStore/_Public/19/100/19100874.pdf
13. Fabbro R, Fournier J, Ballard Devaux PD, Virmont J. Physical study of laser produced plasma in confined geometry. J. Appl. Phys. 1990; 68(2):775. Doi: https://doi.org/10.1063/1.346783
14. Saravanan R, Prema RM. Metal and Alloy Bonding: An Experimental Analysis. Springer-Verlag London Limited, 2012. https://lesezeit.buchkatalog.at/metal-and-alloy-bonding-an-experimental-analysis-9781447122043
15. Abdulzahra NZ, Abood SN. Laser Shock Peening Application as Alternative Method to Determine the Mechanical Properties of Al. Modern Applied Science. 2018; 12(12):102-112. Doi: https://doi.org/10.5539/mas.v12n12p102
16. Abdulzahra NZ. Ultrasonic Shock Wave Generated by Laser as an Alternative Method to Find Different Bone Properties. Lasers in Medical Science. 2023; 38:1381-1395. Doi: https://doi.org/10.1007/s10103-023-03793-3
17. Sugioka K. Laser Precision Microfabrication. Springer-Verlag Berlin Heidelberg, 2010. Doi: https://doi.org/10.1007/978-3-642-10523-4
18. Austin RA, David LD, Benson DJ. Numerical simulation of shock wave propagation in spatially-resolved particle systems. Mater. Sci. Eng. 2006; 14:537. Doi:https://doi.org/10.1088/0965-0393/14/4/001
19. Chaurasia S, Leshma P, Tripathi S, Murali CG, Munda DS, Sharm SM, *et al*. Simultaneous measurement of particle velocity and shock velocity for megabar laser driven shock studies. Barc Newsletter, 2010, 317. https://www.semanticscholar.org/paper/Simultaneous-measurement-of-particle-velocity-and-Chaurasia-Leshma/da653c1cf4ffd84f7f9206563cb8d14d3aaa9756
20. Abdullahi KG, Mamoun M. Laser Peening Process and Its Impact on Materials Properties in Comparison with Shot Peening and Ultrasonic Impact Peening. Materials. 2014; 7:7925-7974. Doi: https://doi.org/10.3390/ma7127925
21. Berthe L, Fabbro R, Peyre P, Tollier L, Bartnicki E. Shock waves from a water-confined laser-generated plasma. J. Appl. Phys. 1997; 82:2826-2832. Doi: https://doi.org/10.1063/1.366113

22. Alwan A, Abdulzahra NZ, Halim NHA. Influence of rapid thermal oxidation process on the optoelectronic characteristics of PSI devices. Int. J. Nanoelectronics and Materials. 2009; 2:157-161. http://dspace.unimap.edu.my/bitstream/handle/123456789/7119/Influence%20of%20rapid%20thermal%20oxidation.pdf?sequence=1
23. Yang B, Zuo J, Tang X, Liu F, Yu X. Effective ultrasound electrochemical degradation of methylene blue wastewater using a nanocoated electrode. Ultrasonics Sonochemistry. 2014; 21:1310-1317. Doi: https://doi.org/10.1016/j.ultsonch.2014.01.008
24. Wang E, Shukla A. Analytical and experimental evaluation of energies during shock wave loading. International Journal of Impact Engineering. 2010; 37(12):1188-1196. Doi: https://doi.org/10.1016/j.ijimpeng.2010.07.003
25. Rienstra SW, Hirschberg A. An Introduction to Acoustics. Rienstra Hirschberg, 2016. https://www.researchgate.net/publication/254911405_An_Introduction_to_Acoustics
26. Grady D. Physics of Shock and Impact, Vol. 1: Fundamentals and Dynamic Failure. IOP Publishing Ltd., 2017. Doi: https://doi.org/10.1088/978-0-7503-1257-8
27. Sundqvist J, Kaplan AFH, Shachaf L, Brodsky A, Kong C, Blackburn J, Assuncao E, *et al*. Numerical optimization approaches of single-pulse conduction laser welding by beam shape tailoring. Optics and Lasers in Engineering. 2016; 79:48-54. Doi: https://doi.org/10.1016/j.optlaseng.2015.12.001
28. Alwan AM, Abdulzahra NZ. The influence of heating treatment on physical properties of porous silicon. Al-Nahrain Journal of Science. 2009; 12(2):76-81. https://anjs.edu.iq/index.php/anjs/article/view/1240/1094
29. Abdulzahra NZ. Laser-Driven Acoustic Waves: Physical Properties of Paramagnetic Metal. Research & Reviews: Journal of Pure and Applied Physics. 2023; 10(6):1-6. Doi: https://doi.org/10.4172/2320-2459.10.6.006
30. Abdulzahra NZ. Extraordinary Magnetoresistance of Laser Annealed Nano Boron Deposited on Oxidized Porous Silicon. Eurasian Physical Technical. 2023; 44:20-31.Doi: https://doi.org/10.31489/2023No2/20-31
31. Angulo I, Cordovilla F, García-Beltrán A, Smyth NS, Anger K, Fitzpatrick ME, Ocaña JL. The effect of material cyclic deformation properties on residual stress generation by laser shock processing. International Journal of Mechanical Sciences. 2019; 156:370-381. Doi: https://doi.org/10.1016/j.ijmecsci.2019.03.029
32. Tambe MJ, Bonini N, Marzari N. Bulk Al at high pressure: A first-principles study. Phys. Rev. B. 2008; 77:172102. Doi: https://doi.org/10.1103/PhysRevB.77.172102
33. Chung Y, Kireev D, Kim M, Akinwande D, Kwon S. Enhanced heat dissipation performance of chemical-doped graphene for flexible devices. Journal of the Korean Physical Society. 2021; 78:45-50. Doi: https://doi.org/10.1007/s40042-020-00014-w